



Health & Safety  
Executive

3277

**OFFSHORE TECHNOLOGY  
REPORT - OTO 98 091**

**Further Assessment of High Strength Steel  
Weld Metals for use in Offshore  
Engineering Applications**

*Date of Issue : April 1998*

*Health & Safety Executive*

This report is made available by the Health and Safety Executive as part of a series of reports of work which has been supported by funds provided by the Executive. Neither the Executive, nor the contractors concerned assume any liability for the reports nor do they necessarily reflect the views or policy of the Executive.

Reports in the OTO series can be obtained from HSE Information Services, Information Centre, Broad Lane, Sheffield S3 7HQ  
Tel: 0541 545500.

**FURTHER ASSESSMENT OF HIGH  
STRENGTH STEEL WELD METALS  
FOR USE IN OFFSHORE  
ENGINEERING APPLICATIONS**

**J.Billingham, S.Blackman & J.Norrish\***  
**Cranfield University**  
**\*now at Wollongong University, Australia**

# **FURTHER ASSESSMENT OF HIGH STRENGTH STEEL WELD METALS FOR USE IN OFFSHORE ENGINEERING APPLICATIONS**

**J. Billingham, S. Blackman, and J. Norrish\***  
**Marine Technology Centre, SIMS, Cranfield University**  
**\* now at Wollongong University, Australia**

## **1. Objectives**

The programme aims to assess the suitability of high strength steel weld metals, at both the 500 and 700MPa strength level, for compatibility with high productivity welding processes currently used in the fabrication of offshore structures. Both SAW and FCAW weld metals will be examined over a range of heat inputs and characterised in terms of microstructure, strength and, particularly, weld metal toughness. The corrosion fatigue crack propagation behaviour of the weld metals in seawater under different levels of applied cathodic protection will be examined to assess their suitability for likely in-service performance. Particular emphasis will be placed on determining the most suitable microstructure to ensure satisfactory toughness and weldability and in-service corrosion fatigue requirements. In addition, the suitability of GMAW consumables for welding X80 and X100 grade (550 and 694MPa) linepipe will also be examined and their weldability, weld quality and impact performance assessed.

## **2. Introduction**

Most offshore structures contain considerable quantities of weldable structural steels with yield strengths up to 350MPa. High strength steels have traditionally been used in the offshore engineering industry in pipelines<sup>(1)</sup>, typically grades X65 - X70 (455 - 480MPa), and in jack-ups<sup>(2)</sup> where steel with strength up to 700MPa has been utilised. More recently there has been a considerable growth in the amount of higher strength steels used in jacket structures, primarily to save weight and cost<sup>(3)</sup>. With the evolution of heavy lift crane barges, lift installed platforms have been increasingly attractive compared to barge loaded structures and this has brought about considerable efforts to minimise structural weight by optimising design, platform layout and topside equipment. The use of high strength steels, principally grades 420 and 460, have played a major role in this and the amount of such steel used in these structures has increased from 8% in 1988 to 40% in 1995<sup>(4)</sup>. Most current applications are limited to topsides, but increasingly other parts of the jacket are also utilising such materials.

Additional benefits of using high strength steels are derived in the fabrication yard since significant time and cost savings can be achieved through the use of thinner

sections and reduced weld volumes, and the possibility of reducing or avoiding PWHT in some cases<sup>(5)</sup>.

The use of 450MPa yield strength steels is now well established and recent reviews at Cranfield<sup>(4)</sup> and elsewhere<sup>(6)</sup> have confirmed the suitability of such steels provided that certain requirements are satisfied in terms of composition and alloy type. Other work at Cranfield has confirmed the promise of even higher strength steels with yield strengths of 550MPa<sup>(7)</sup>. Other workers have confirmed that 700MPa steels have suitable properties for use in submarines and jack-ups for use in marine environments<sup>(8)</sup>.

However, although suitable steels are available and can demonstrate satisfactory HAZ performance after welding, much less attention has been given to the development and performance of the associated weld metals for such applications. Work at Cranfield within the previous Managed Programme<sup>(7)</sup> confirmed the experience of the fabrication industry that at the 450MPa strength level the steels are readily weldable without undue precautions and that at the 550MPa level, satisfactory weld performance could be achieved. Satisfactory performance was closely associated with the type of weld metal microstructure produced, high levels of acicular ferrite, small grain size and low levels of grain boundary ferrite all being favoured.

The two main welding processes of interest to the offshore fabrication industry, from a productivity view point, are submerged arc (SAW) and flux cored arc welding (FCAW). SAW because of its proved reliability to produce consistent weld metal with good mechanical properties and the ability to increase the deposition rates through metal powder additions and multiple wire welding, and FCAW mainly because of its positional welding capabilities. Hence, the development of suitable SAW and FCAW consumables with excellent strength and toughness for welding HSLA steels is of major interest to the offshore fabricators.

Weld metal microstructures are determined primarily by the chemical composition, the amount of non-metallic inclusions present in the microstructure which affect phase nucleation, and by the cooling rate. Alloy design aims to maximise the amount of acicular ferrite present and to minimise the effects of undesirable microstructures such as coarse grain size, grain boundary ferrite and coarse MAC.

The welding consumables employ sophisticated alloying techniques, incorporating the optimum balance of deoxidising elements (aluminium, silicon and manganese) to produce a high density of small non-metallic inclusions which are known to act as intragranular nucleation sites for acicular ferrite. The carbon content is generally kept low to aid weldability, so the increased strength is achieved through additions of molybdenum in SAW wires and titanium-boron in FCAW wires, and the impact toughness is improved with nickel additions. Indeed, Zhang and Farrar<sup>(9)</sup> recently suggested that a combination of 0.6 - 1.4 manganese and 1.0 - 3.7% nickel was needed for optimum toughness. Molybdenum and nickel have the effect of suppressing the pro-eutectoid ferrite formation below that of acicular ferrite, hence making a more favourable growth regime for acicular ferrite. A small amount of

titanium has been found to increase the acicular ferrite content ten-fold, while the boron segregates to the grain boundaries preventing the formation of grain boundary ferrite<sup>(10)</sup>. The level of oxygen in the weld metal also influences the microstructure, its main effect being related to the volume fraction, size distribution, and type of oxide products formed<sup>(11)</sup>.

High productivity is necessary to ensure maximum cost benefits in construction and one way of achieving this is to improve the welding deposition rates, and hence shorten the joint completion times during welding. A test programme was therefore devised in order to investigate how currently available 550 and 700MPa yield strength high strength steels SAW and FCAW consumables behave under high productivity situations.

The recent emphasis on cost reduction in offshore activities has led to increased attention to the potential benefits of using higher strength steel for pipeline applications. An additional study was therefore initiated to examine the weldability and toughness of GMAW pipeline welding consumables suitable for welding X80 (550MPa) and X100 (694MPa) linepipe.

If high strength steels are to be used in offshore engineering jacket structures they must be resistant to corrosion fatigue. Previous work has examined the corrosion fatigue and propagation behaviour of high strength steels<sup>(12)</sup> and their HAZs after welding and found generally satisfactory properties<sup>(13)</sup>. However, there is very little data in the literature on the performance of their associated weld metals. The proposed programme aimed to address this deficiency.

### **3. Experimental**

Two HSLA steels were chosen for use in this programme; RQT501 (550MPa) from British Steel, and Weldox 700 (700MPa) from Svenskt Stal, both in the quenched and tempered condition. Two SAW consumables were chosen for welding RQT501; SD3iNi $\frac{1}{2}$ Mo from Oerlikon, and Tubrod 14.54, a tubular wire of similar composition from ESAB. Two similar strength FCAW consumables were also examined; Corofil B65 a basic wire from Murex, and TM-881-K2 a recently developed rutile wire from Oerlikon. For welding the 700MPa steel, the SAW consumables used were Tubrod 14.55 from ESAB and Fluxocord 42 from Oerlikon, and the FCAW consumables were Dual Shield II-120M2 from Alloy Rods and Fluxofil 42 from Oerlikon. All consumables were currently available from recognised manufacturers. Details of the alloy compositions and mechanical properties are given in Table I.

Single 'V' butt welded joint configurations with 60° included angle, backing plate, and suitable restraint were used to create similar conditions to those used when welding offshore fabrications. For the SAW trials nominal heat inputs of 3.5kJ/mm (the current limit for offshore fabrications) and 6kJ/mm (to observe what happens when an attempt is made to raise productivity) were used. For the FCAW trials, 0.7 and 2kJ/mm were used to study the effect of the different heating and cooling regimes on the weld metal microstructures and mechanical properties.

Full thickness sections from each weldment were polished to a 1 $\mu$ m finish and etched in 2% nital to reveal the ferritic microstructure for observation under the optical microscope. The quantities of various microstructural constituents were measured in the last weld beads deposited using a Swift point counter following the procedure described in IIW Doc. II-A-389-76<sup>(14)</sup>. Vickers hardness traverses across the cap, mid-thickness, root and down the weld centre line were carried out at 2mm intervals using a load of 10kg. All-weld-metal longitudinal tensile test pieces were machined from the cap and root centre line regions and tested using a Nene testing machine with a 30kN maximum load and a strain rate of 0.5mm/s. Load versus displacement curves were plotted automatically, and the yield and ultimate tensile strengths calculated accordingly.

Ten standard Charpy V-notch specimens (10 x 10 x 55mm) were extracted from the cap and root regions of each weldment and notched on the weld centre line in the T-L orientation. The specimens were fractured at temperatures which ranged from room temperature to -80°C, and full transition curves were plotted. In an attempt to correlate the impact properties with the microstructures in the weld metals, the types of microstructural phases (columnar, coarse, and fine grained) along the notch were measured using the Swift point counter, so it was possible to observe which microstructure influenced the impact properties. Deposited weld metal compositions were determined by direct spark analysis using a Quantovac 34000 optical emission spectrometer. Oxygen and nitrogen contents were determined using a Leco analyser.

For the corrosion fatigue test programme 50mm thick high strength steel plates were welded at a heat input between 1.5 and 2kJ/mm using both the SAW and FCAW processes with a 60°V preparation and a backing plate using preheat and interpass temperatures of 120 and 150°C respectively. Standard 3 point bend tests were used, surface notched at the centre of the weld deposit with the cracks running in the short transverse direction (through thickness). Prior to precharging and testing of the weld metal specimens, a fatigue precrack was grown in-air in the specimens at a frequency of 10Hz using a reducing load method.

Corrosion fatigue crack propagation tests (Paris tests) were carried out using constant amplitude cycles of high mean stress ratio ( $R = 0.6$ ) and a test frequency of 0.5Hz to allow comparison to in-service behaviour and the earlier Cranfield high strength steel test programmes<sup>(4,7,13)</sup>. Duplicate tests were carried out for each test condition of applied cathodic potential on each weld metal. Crack growth was monitored and recorded using an alternating current potential drop (AC-PD) measuring system and an optical travelling microscope.

Test data in the form of crack length as a function of number of cycles was recorded and converted into the standard  $da/dN$  versus  $\Delta K$  format incorporating an ASTM 7 point polynomial analysis technique. Post-test evaluation using optical and scanning electron microscopy was used to determine the fatigue failure mechanisms. In all experiments reported in this study, an 8 week hydrogen precharging period was

used prior to testing. This was considered to be a severe test when compared to most other data reported in the literature.

For the pipeline welding programme, 5 GMAW consumables were selected for investigation. All tests were performed at 0.8kJ/mm heat input and the weld preparation and test methods were designed to avoid dilution effects from the parent material. The work looked at the effect of shielding gas and transfer mode on the mechanical properties of the deposited weld metals in order to determine their suitability for welding high strength linepipe. Table II provides a summary of the welds produced. After reviewing the initial trials with CO<sub>2</sub> shielding gas in the dip transfer mode, only 3 consumables (Carbofil H7, Union NiMoCr and Bohler X70-1G) were selected for further trials using both pulsed and dip transfer and a number of different shielding gas.

## **4. Results and Discussion**

This section is divided into 3 parts; firstly the examination of the 550 and 700MPa structural offshore welds in terms of both microstructure and mechanical properties especially notch ductility, secondly the examination of the corrosion fatigue crack propagation performance of the 550 and 700MPa weld metals, and finally the examination of the X80 (550MPa) and X100 (694MPa) pipeline consumables.

### **4.1 Metallurgical Examination of 550 and 700MPa Weld Metals**

All the consumables examined produced sound welds which were defect-free and had microstructures consisting of largely acicular ferrite together with smaller amounts of pro-eutectoid ferrite and ferrite side plate structures as shown in Figures 1 and 2. The multi-pass welds contained large amounts of reheated microstructures. In the coarse grained reheated region ferrite formed at the columnar grain boundaries and the fine grained regions were largely composed of ferrite microstructures.

The average hardness of the welds ranged from 200 in the 550MPa welds to 240HVN in the 700MPa welds. Maximum hardness values were 238 at 550MPa and 312HVN at 700MPa which were below values at which cold cracking would be expected to pose problems and no cold cracking was observed. Tensile testing revealed that the welds usually overmatched the specified yield strength values by 5 - 20% although one or two welds, Corofil B65 TM881-K2 and DualShield 120 undermatched the parent by up to 10%. All welds, however, exhibited good ductility (>20%). A summary of the mechanical properties is given in Table III.

The lower bound impact transition curves for the SAW550 weld metals are shown in Figure 3. Generally there was little scatter between tests, indicating sound weld metal and homogenous microstructures. In general, both room temperature and low



temperature impact performance were good, a target 55J impact energy at -40°C being achieved. There was little difference between the 3.5 and 6.0kJ/mm welds.

The FCAW weld metal results are shown in Figure 4. Generally the notch ductility is excellent with -40°C values of over 100J but the Corofil NQ1 consumable properties were reduced in the root region at 1.7kJ/mm.

The lower bound impact energy curves for the 690MPa SAW weldments are shown in Figure 5. The properties for Fluxocord 42 are generally quite good, although the properties do decrease somewhat at the highest heat input. The properties of Tubrod 14.55 are generally excellent in the root specimens but the cap values show a significant reduction in properties which was associated with coarsening of the microstructures. The 70J at -40°C requirement was only achieved in the root regions of the Tubrod welds. The microstructures produced were a mixture of fine acicular ferrite and regions of martensite and bainite. There was no excessive grain coarsening and the microstructures were fairly uniform. Figure 6 shows the 700MPa FCAW impact transition curves. Slightly better properties were achieved in the root region of both welds. Fluxofil 42 contained fine acicular ferrite and martensite whereas Dual Shield contained acicular ferrite and some ferrite side plate microstructures. The variations in the amounts of reheated microstructure in different samples made correlations of microstructure with mechanical properties very difficult. In general, however, the FCAW samples contained larger amounts of acicular ferrite as deposited and retained their fine grained structure better on heating.

Detailed chemical analyses indicated little variation in chemical composition between cap and root regions but indicated that the oxygen levels varied from 200 - 400ppm in the SAW and between 400 - 600ppm for the FCAW. In SAW welds inclusion size increased as the heat input increased but inclusion volume fraction usually decreased because the corresponding oxygen content in the weld was reduced. Low toughness values were found to correlate with large inclusion sizes and the best impact properties were found with inclusion sizes varying from 0.4 to 0.6µm, corresponding to intermediate levels of oxygen of 200 - 400ppm. In FCAW the inclusion sizes were smaller but the volume fractions were larger because of the high oxygen levels. The inclusion species did not change significantly over the range of heat inputs investigated, leading to an abundance of inclusions to nucleate acicular ferrite microstructures and give good impact properties.

An attempt was made to utilise weld metal models developed by Dr. H. Bhadeshia at Cambridge University for carbon manganese structural steel welds and extend them to the higher strength weld metal materials used in this programme. The model uses the weld metal composition and welding parameter data as input requirements, and uses known transformation behaviour to predict weld metal microstructures and hence the resulting mechanical properties.

The computer model usually overestimated the strength of the weld metal as shown in Figure 7. Model predictions were closest for the 450MPa strength weld metals and worst for the highest strength 690MPa welds. In general, the agreement was

closer for the ultimate strength values than for the yield strength values. For the 450MPa welds the model gave excellent predictions which were usually within 5% for the UTS values and 10% for the yield strength values which was expected because the microstructures were similar to those of lower strength structural steel for which the models had been developed. The model also gave closer agreement for the FCAW welds than for the SAW welds, and it also gave better agreement for the root regions than for the cap regions in the SAW. These observations indicated that the model was underestimating the loss in strength in the cap region due to grain coarsening at the highest heat input values used which were greater than those commonly specified. Attempts to use simple models to predict impact behaviour gave very poor correlation with actual experimental results.

## 4.2 Corrosion Fatigue Crack Propagation Behaviour

The corrosion fatigue crack propagation behaviour of the SAW and FCAW high strength steel weld metals is shown in Figures 8 and 9 for the 550 and 700MPa consumables examined in this programme. It can be seen from the crack length against number of cycles plots in Figure 8 that the crack growth rates at -1100mV (Ag/AgCl) are considerably faster than the rates at -850mV. In the conventional Paris plot shown in Figure 9 it can be seen that cracks grew some 2 to 5 times faster at -1100mV than at -850mV and the curves are much flatter at the higher potential, indicating that hydrogen embrittlement is playing a significant role in the failure process. It can be seen that neither welding process (SAW, FCAW) or steel strength (550, 700MPa yield strength) produce significant difference in performance in these corrosion fatigue experiments. This indicates that the differences in composition and microstructure between the welds did not have a significant effect on crack propagation rate, reinforcing earlier work by Laws and Billingham<sup>(15)</sup>. The results compare favourably with published work by King<sup>(12)</sup> on high strength steels and with heat affected zone performance in earlier published work by Cranfield<sup>(13)</sup> under similar conditions of applied cathodic potential as shown in Figure 10. It can be seen from these diagrams that the high strength weld metals show satisfactory fatigue performance compared to both published data from high strength steels and compared to the BS6493 mean lines.

There is little published data on the corrosion fatigue behaviour of high strength weld metals but both Zang<sup>(16)</sup> and Todd<sup>(17)</sup> indicate that 500 and 590MPa weld metals show comparable crack propagation rates to conventional 350MPa C-Mn-50D steel. Cranfield has recently carried out a separate study on a number of high strength steel weld metals for the Health and Safety Executive which will be published shortly<sup>(18)</sup>.

These results are encouraging because they indicate that high strength weld metals are unlikely to be a source of enhanced fatigue crack growth behaviour in high strength steel structures in marine environments because they show comparable, or even slightly improved, fatigue crack propagation behaviour compared to their parent high strength steels and their associated heat affected zones. Moreover,

they show slightly improved behaviour to conventional carbon manganese structural steels (~350MPa) currently widely used offshore.

### 4.3 Properties of High Strength Pipeline Weld Metals

Several of the consumables tested exhibited a satisfactory combination of strength, weldability and notch ductility for the proposed subsea pipeline application. In the dip transfer mode Argoshield 20 gave the highest impact energy with Carbofil HT and Bohler X70-1G consumables, whereas TIME gas was the best shielding gas used with Union NiMoCr. Using pulsed mode operations, Trimix gas provided the best impact properties for Carbofil HT and Bohler, whereas again TIME was the best option for Union NiMoCr. In most cases the use of pulsed mode gave better impact properties than dip mode. This agrees with results obtained by Laing<sup>(19)</sup>. Figure 11 shows the effect of varying shielding gas and transfer mode for the Union NiMoCr consumable. The best properties were obtained with TIME gas in the pulsed mode although all shielding gases gave satisfactory performance using pulsed transfer.

The results obtained with different shielding gases for both dip and pulsed mode showed that, with all consumables, an increase in the oxygen content of the gas caused a decrease in both maximum and average weld metal hardness. These trends are in agreement with previous literature. In their previous works, Ito<sup>(20)</sup>, Lathabai<sup>(21)</sup> and, more recently, Onsøien<sup>(22)</sup>, using argon/CO<sub>2</sub> mixtures, concluded that, in most cases, increasing levels of oxygen in the shielding gas led to a decrease in weld metal hardness. The explanation given by them is based on the fact that increasing oxygen in the gas affects manganese and silicon levels which, in turn, will change the hardenability of the weld metal. Because manganese and silicon are strong deoxidizers they tend to react with oxygen during welding and with increasing levels of oxygen in the gas greater loss of these elements is expected. However, the trends in silicon and manganese content in the actual weld deposits were not consistent.

In general, ultimate tensile strength has a behaviour similar to hardness, i.e. increasing levels of oxygen in the shielding gas lead to a small decrease in ultimate tensile strength. These results are in agreement with previous work by Church<sup>(23)</sup> and Ito<sup>(24)</sup>.

There was not a clear trend linking yield strength with oxygen in the shielding gas but in most cases, lower values of yield strength were observed when comparing pulsed transfer with dip transfer. Carbofil HT had the lowest yield strength and in some instances failed to satisfy the SMYS of 690MPa for X100 grade linepipe. Union NiMoCr had the highest yield strength and in some cases exceeded 828MPa which would satisfy X120 requirements.

## 5. Conclusions

1. Both SAW and FCAW 550MPa consumables showed excellent impact properties with upper shelf values >150J and 50J impact transition temperatures below 60°C. Several consumables produced satisfactory properties.
2. In 550MPa welds acicular ferrite was the major microstructural feature found but proeutectoid ferrite and ferrite side plates also occurred. Microstructures generally coarsened as heat input increased, especially for the SAW welds at very high heat input. Hardness values were usually low and no hydrogen cracking problems are envisaged. In SAW inclusion size increased as heat input increased and low notch ductility was associated with large inclusion size. In FCAW the inclusion size was smaller but the volume fraction increased because of the higher oxygen levels, leading to easier nucleation of acicular ferrite and good impact properties.
3. For SAW and FCAW 690MPa consumable mixed microstructures containing fine acicular ferrite, martensite and polygonal ferrite were obtained. Impact properties were not as good as the the 550MPa welds with lower shelf energies ranging from 80 - 100J and 50J transition temperatures between -50 and -80°C. More development work is required on these higher strength consumables before they can safely be specified generally for offshore application.
4. Computer models are available which can give good predictions of yield strength for 450MPa weld metals ( $\pm 10\%$ ), and for ultimate tensile strength ( $\pm 5\%$ ). The models were much less reliable for higher strength welds (550 and 690MPa), usually over-predicting by as much as 30%. Model predictions for impact performance are currently very poor.
5. With appropriate selection of welding consumables, shielding gas, and transfer mode, it was possible to deposit weld metal with excellent notch ductility and strength in excess of the requirement for X80 and X100 linepipe. Welding with pulsed transfer mode gave improved impact toughness properties. In fact, with one consumable, the results exceeded the requirements for X120 linepipe.
6. High strength steel weld metals show comparable corrosion fatigue behaviour in sea water to their respective parent materials at the same strength level, and slightly better performance than lower strength structural steels.
7. High negative applied potentials led to an acceleration in crack growth rates (2 to 5 times faster at -1100mV than at -850mV). At -1100mV, especially for the 700MPa welds, the curves became flatter, indicating that hydrogen embrittlement was playing a major role in the failure process.

8. These results are encouraging, indicating that high strength steel weldments are unlikely to be a source of enhanced fatigue crack growth in marine structures.

## 6. Future Work

1. Further work is required to develop high strength welding consumables that can be welded under high productivity welding conditions to produce weldments of high strength and good impact performance. In particular, a more extensive metallographic study is required to examine the metallurgical influences of compositional modifications on phase nucleation and growth. More attention could be paid to ultra-low carbon bainitic weld metals.
2. This preliminary study has indicated that suitable high strength pipeline consumables do exist provided that the welding process is carefully controlled in terms of shielding gas and transfer mode. Further work is required to look at the effect of parent metal dilution and HAZ performance, particularly for X100 operations before safe recommended procedures can be specified.

## REFERENCES

1. *Gray J M*, 'Alloy Design - Options and Compositional Trends for HSLA Line Pipe', Proc. Microalloying 88, Chicago, publ. ASME 1988.
2. *Sharp J V, Billingham J, and Stacey A*, 'Performance of High Strength Steels Used in Jack-ups', 6<sup>th</sup> Intl. Conf., The Jack-up Platform, London 1997, AST Press.
3. *Billington C J*, 'Application of High Strength Steels in Fixed Offshore Platforms', conf. Safe Design and Fabrication of Offshore Structures, London 1993, publ IBC.
4. *Billingham J, Healy J, and Spurrier J*, 'Current and Potential Use of High Strength Steels in Offshore Structures' Publication 95/102, Marine Technology Directorate, London, 1995.
5. *Rodgers K J, and Lockhead J C*, 'Welding of Grade 450 Offshore Structural Steels', Proc. conf. on Welding and Weld Properties in the Offshore Industry, London 1992, Publ IBC.
6. *Stacey A, Sharp J V, and King R N*, 'High Strength Steels Used in Offshore Installations', OMAE 1996, Vol.III, p417, Publ. ASME.
7. High Strength Steels in Offshore Engineering, MTD Publication 95/100, London 1995.
8. *Bennett W T Jr, Cadiou L, and Caudreuse L*, 'Steels for Jack-up Legs' in Recent Developments in Jack-up Platforms, ed. Boswell L F and D'Mello C, Blackwell 1992.
9. *Zhang Z, and Farrar R A*, Welding Research Supplement May 1997, 183S.
10. *Evans G M*, 'The Effect of Microalloying in C-Mn Steel Weld Metals', Welding in the World, 41, 1, 1993, 12.

11. *Dowling J M, Corbett J M, and Kerr H W*, 'Inclusion Phases and Nucleation of Acicular Ferrite in Submerged Arc Welds in High Strength Low Alloy Steels', *Met. Trans., A*, Vol.17A, 1986, 1611.
12. *King R N, Stacey A, and Sharp J V*, 'A Review of Fatigue Crack Growth Rates for Offshore Steels in Air and Seawater Environments', *OMAE 1996*, Vol.III, 341, Publ.ASME 1996.
13. *Healy J, Billingham J, Stacey A, Simpson R, and Patel R*, 'Review of Corrosion Fatigue Performance of Medium to High Strength Steels', *OMAE 1996*, Vol.III, Mats. Eng. 451, Publ. ASME 1996.
14. *Davey T G, and Widgery D J*, 'A technique for the characterisation of weld metal microstructures', *Inst. of Welding, Doc.11, A 389-96*, 1976.
15. *Billingham J, and Laws P*, 'High Fatigue Crack Propagation in High Strength Steels For Use Offshore', *OMAE 1994*, Vol.III, p129, publ. ASME.
16. *Zang Q*, 'Corrosion fatigue crack growth rate of A537 steel and to weld metal in artificial seawater', *Proc.Intl.Conf. on Corrosion and Corrosion Control for Offshore and Marine Construction*, 1988, Xiamen, China, 131.
17. *Todd J A*, 'A comparison of the near threshold corrosion fatigue crack propagation rates of MILS 24645 HSLA steel and its weldments',
18. Private Communication, Cranfield and HSE, to be published in *OMAE 1998*.
19. *Laing B S*, 'PGMAW welding of X80 pipe', *Proceedings of the Offshore Pipeline Technology Conference*, Feb. '90, Paris, France.
20. *Ito Y*, 'Effects of oxygen on low carbon steel weld metal', *Metal Construction*, Sept. '82, pp472-478.
21. *Lathabai S, and Stout R*, 'Shielding Gas and Heat Input Effects on Flux Cored Weld Metal Properties', *Welding Journal*, Nov. '85, pp303s-313s.
22. *Onsøien M I*, 'Shielding Gas Oxygen Equivalent in Weld Metal Microstructure Optimisation', *Welding Journal*, July '96, pp216s-224s.
23. *Church J*, 'Welding characteristics of a new welding process', *Time Process*, IIW doc.No.XII-1099-90, 1990, pp1-73.

**TABLE I - Chemical Compositions and Mechanical Properties of Weld Metals Used in the Programme**

| Weld Metal Designation | Type | Manufacturer | Composition |      |      |      |      |      |      | Yield Strength (MPa) |
|------------------------|------|--------------|-------------|------|------|------|------|------|------|----------------------|
|                        |      |              | C           | Mn   | Si   | Ni   | Mo   | Cr   |      |                      |
| SD3 1Ni ½Mo            | SAW  | Oerlikon     | 0.10        | 1.6  | 0.23 | 0.98 | 0.58 |      | 645  |                      |
| Tubrod 14.54           | SAW  | ESAB         | 0.07        | 1.6  | 0.2  | 1.3  | 0.5  |      | 580  |                      |
| Carofil NQ1            | FCAW | Murex        | 0.05        | 1.3  | 0.4  | 1.0  |      |      | 620  |                      |
| TM881-K2               | FCAW | Oerlikon     | 0.06        | 0.98 | 0.24 | 1.41 |      |      | >560 |                      |
| Corofil B65            | FCAW | Murex        | 0.06        | 1.6  | 0.4  | 1.5  |      |      | 560  |                      |
| Fluxofil 42            | FCAW | Oerlikon     | 0.05        | 1.3  | 0.35 | 2.4  | 0.4  | 0.4  | >690 |                      |
| Dual Shield            | FCAW | Alloy Rods   | 0.03        | 1.77 | 0.25 | 2.72 | 0.01 | 0.03 | 698  |                      |
| Tubrod 14.55           | SAW  | ESAB         | 0.07        | 1.6  | 0.4  | 2.8  | 0.3  |      | 710  |                      |
| Fluxocord 42           | SAW  | Oerlikon     | 0.05        | 1.4  | 0.2  | 2.5  | 0.4  | 0.6  | >680 |                      |

**TABLE II - Summary of Tests Carried Out in High Strength Pipeline Weld Metal Test Programme**

| <b>Welding Consumables</b> | <b>Shielding Gas and Metal Transfer Mode</b> |                                   |                              |                                      |                               |                                 |
|----------------------------|--|-----------------------------------|------------------------------|--------------------------------------|-------------------------------|---------------------------------|
|                            | <b>CO<sub>2</sub> Dip Transfer</b>           | <b>Argoshield 20 Dip Transfer</b> | <b>Time gas Dip Transfer</b> | <b>Argoshield 20 Pulsed Transfer</b> | <b>Trimix Pulsed Transfer</b> | <b>Time gas Pulsed Transfer</b> |
| Oerlikon<br>Carbofil HT    | 1A   | 2A                                | 3A                           | 4A                                   | 5A                            | 6A                              |
| Thyssen<br>Union NiMoCr    | 1B   | 2B                                | 3B                           | 4B                                   | 5B                            | 6B                              |
| Bohler X70-1G              | 1C   | 2C                                |                              | 4C                                   | 5C                            |                                 |
| Thyssen<br>Union X85       | 1D   |                                   |                              |                                      |                               |                                 |
| Bohler NiMo 1G             | 1E   |                                   |                              |                                      |                               |                                 |



**TABLE III - Summary of Mechanical Properties of the Deposited Weld Metals**

| Process | Strength Level (MPa) | Wire         | Heat Input (kJ/mm) | YS (MPa) | UTS (MPa) | CV@ -40°C (J) |
|---------|----------------------|--------------|--------------------|----------|-----------|---------------|
| SAW     | 550                  | Tubrod 14.54 | 1                  | 662      | 717       | 61-145        |
|         |                      | SD31Ni ½ Mo  | 6                  | 588      | 674       | 76-104        |
|         | 690                  | Tubrod 14.55 | 3.5                | 664      | 752       | 77-127        |
|         |                      |              | 6                  | 659      | 765       | 56-130        |
|         |                      | Fluxocord 42 | 3.5                | 742      | 829       | 41-103        |
|         |                      |              | 6                  | 756      | 756       | 42-115        |
| FCAW    | 550                  | Corofil NQ1  | 3.5                | 751      | 865       | 60-108        |
|         |                      |              | 6                  | 785      | 961       | 64-73         |
|         |                      |              | 0.7                | 620      | 659       | 92-156        |
|         | 690                  | TM-881-K2    | 1.8                | 548      | 596       | 52-149        |
|         |                      |              | 0.7                | 531      | 587       | 113-128       |
|         |                      |              | 1.7                | 507      | 574       | 113-145       |
| 690     | Dual Shield 120      | 1.7          | 504                | 591      | 108-133   |               |
|         |                      | 1.7          | 754                | 871      | 61-81     |               |
|         |                      |              |                    |          |           |               |
|         |                      |              |                    |          |           |               |

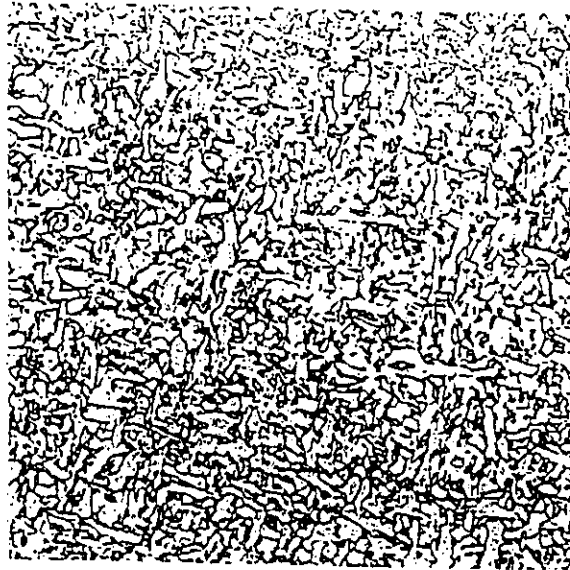


**FIGURE 1** Showing acicular ferrite in SD1Ni ½ Mo SAW 550MPa weldment.  
Etched in 2% nital

x600

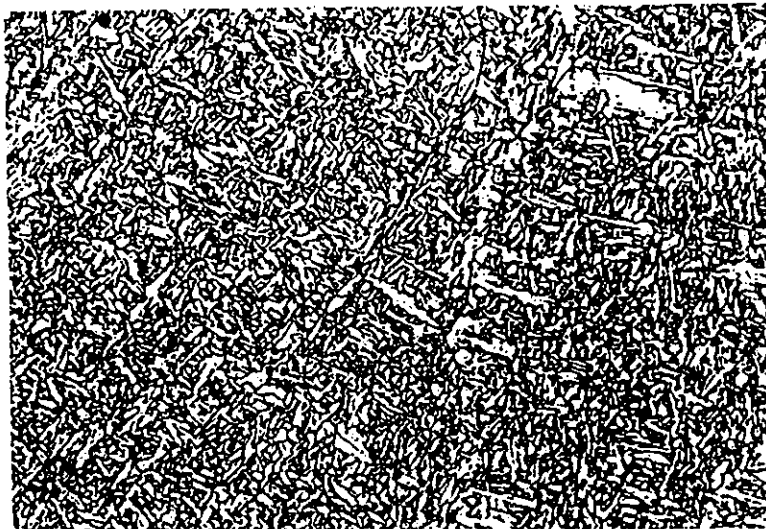


**FIGURE 2** Showing acicular ferrite in TM881-K2 FCAW 550MPa weldment.  
Etched in 2% nital

x400

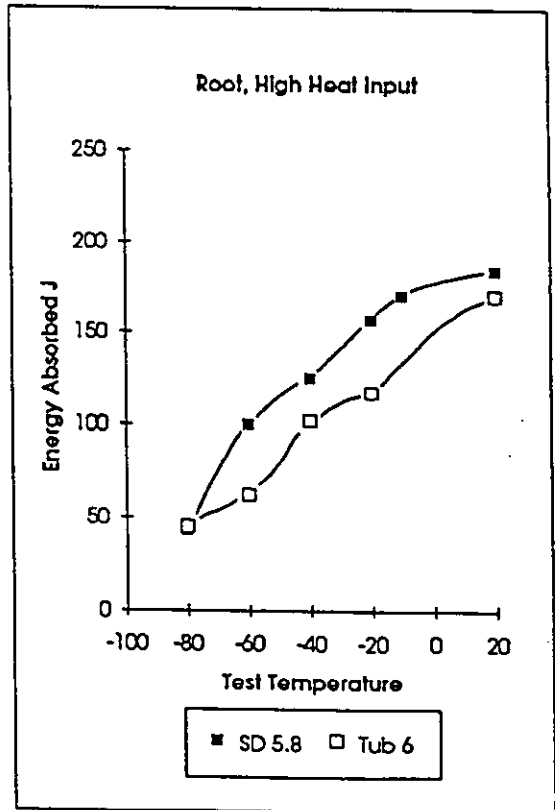
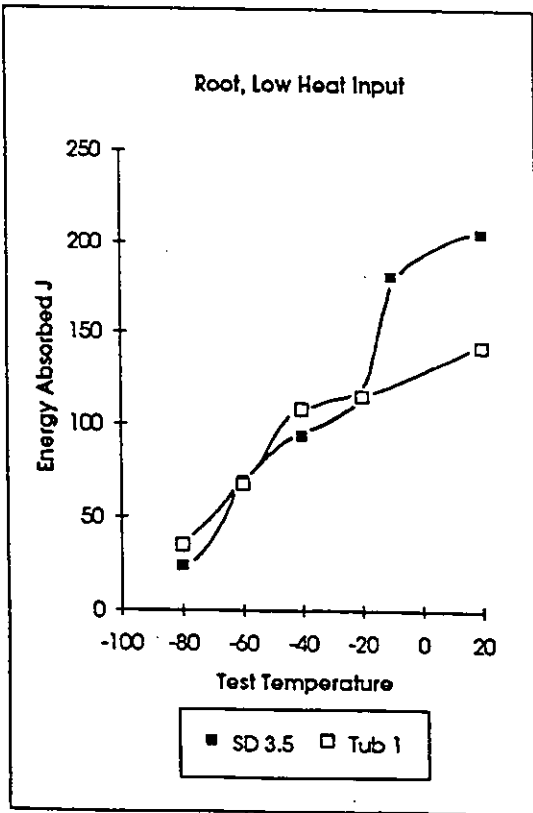
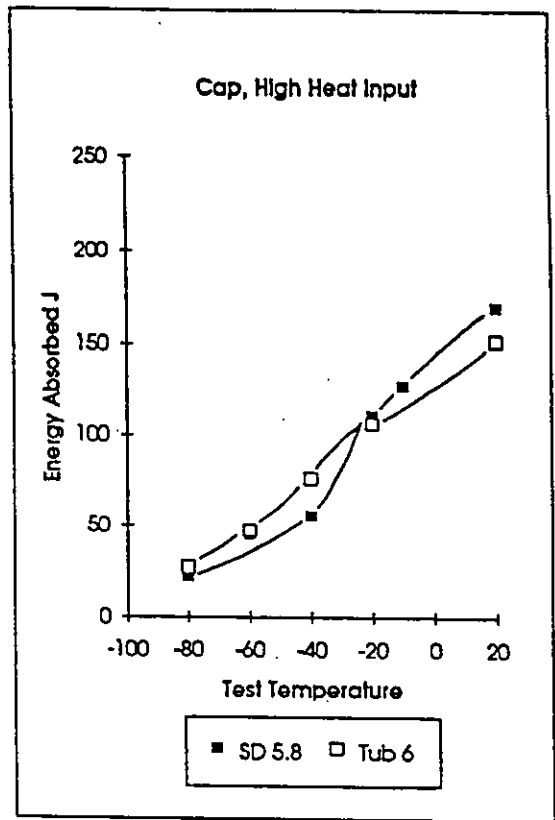
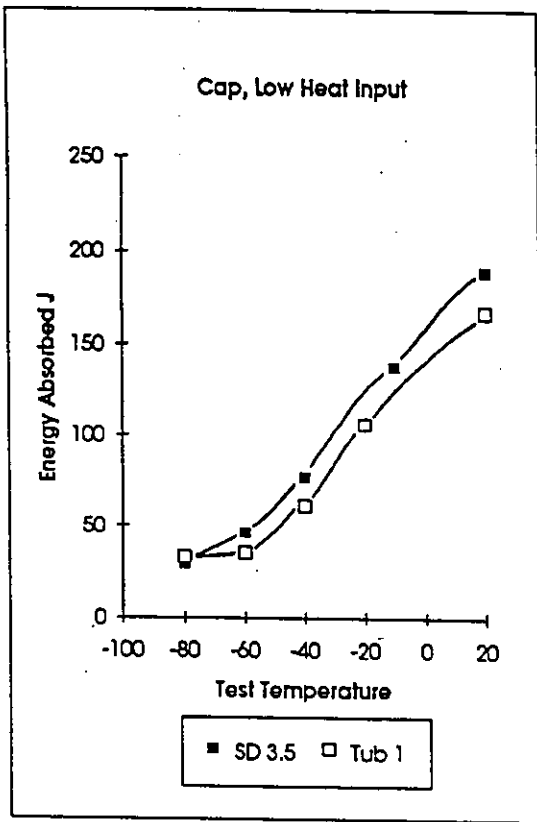


**FIGURE 3** Showing lower bound Charpy-V Notch Impact Transition Curves for the 550MPa yield strength SAW welds SD31Ni ½Mo and Tubrod 14.54

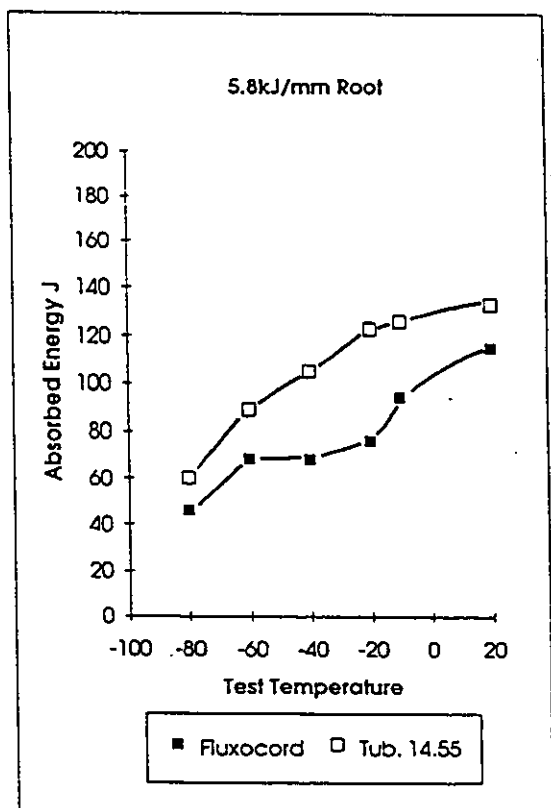
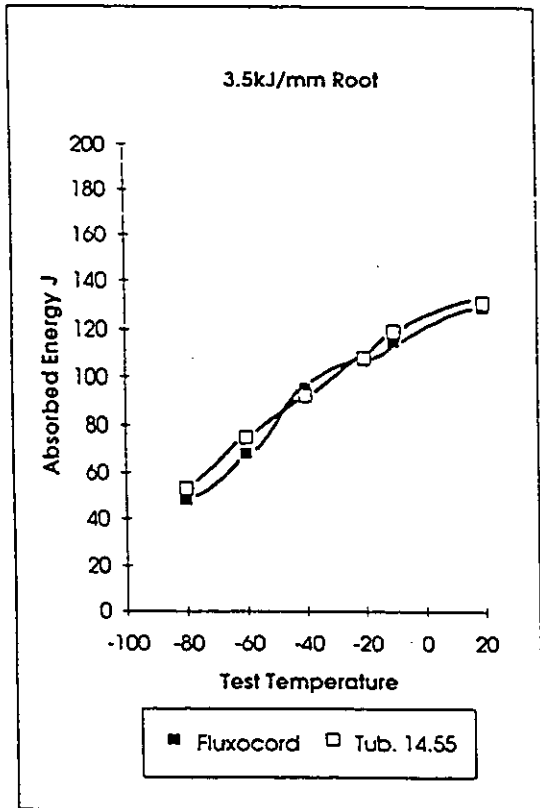
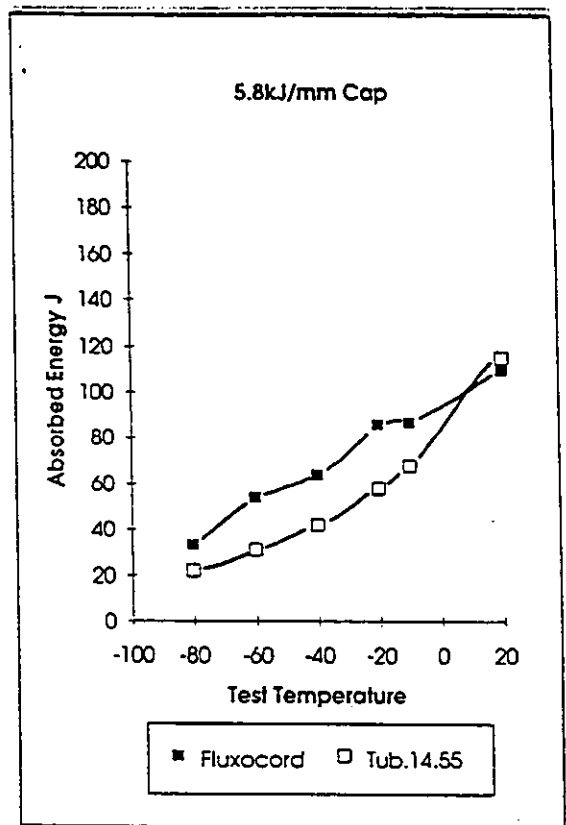
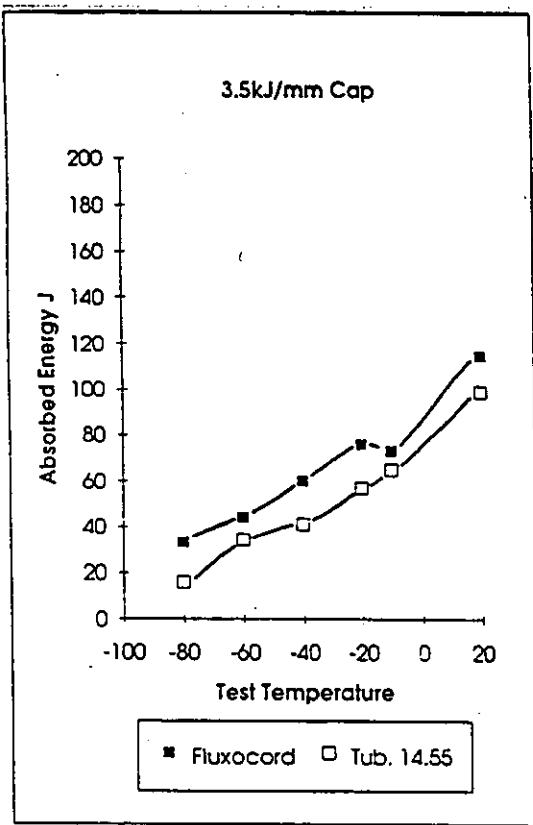


**FIGURE 5** Showing lower bound Impact Transition Curves for the 690MPa yield strength SAW welds Tubrod 14.55 and Fluxocord 42

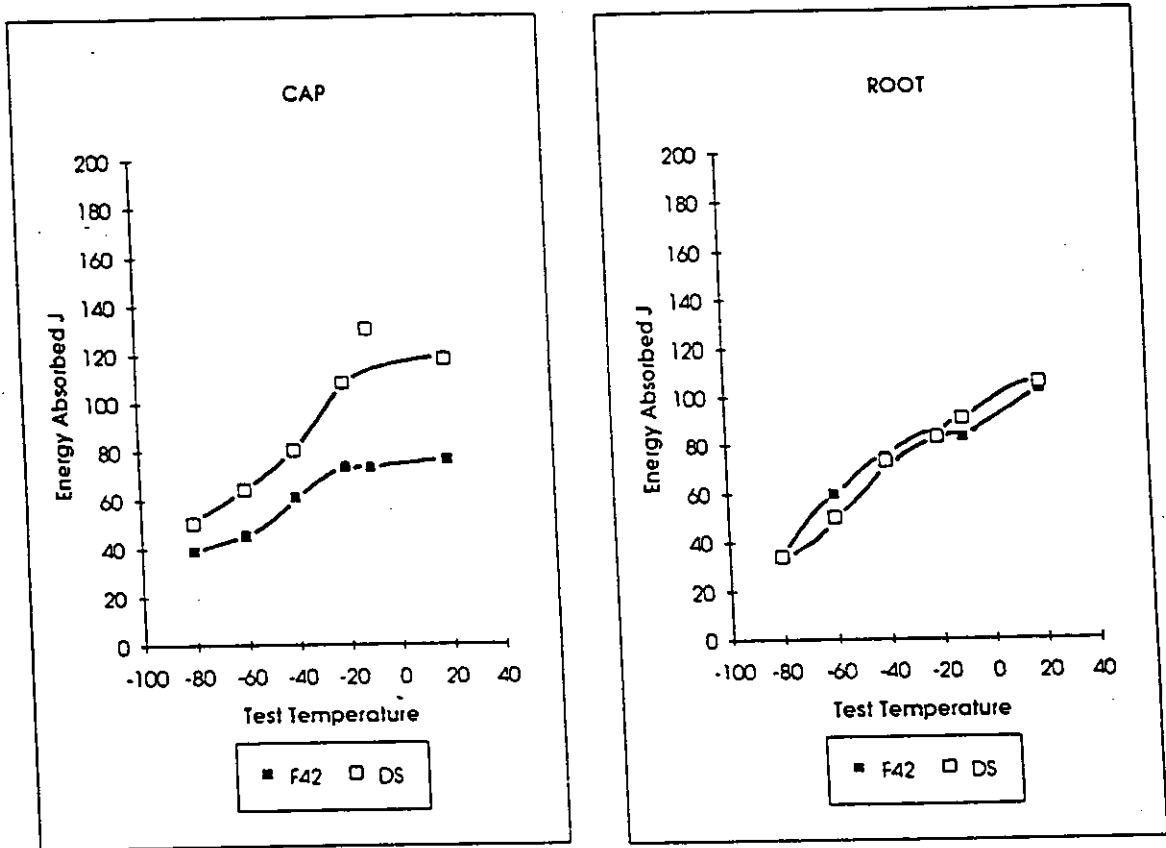


**FIGURE 6** Showing lower bound Charpy-V Impact Transition Curves for the 690MPa yield strength FCAW welds Fluxofil 42 and Dual Shield 120 at 1.7kJ/mm

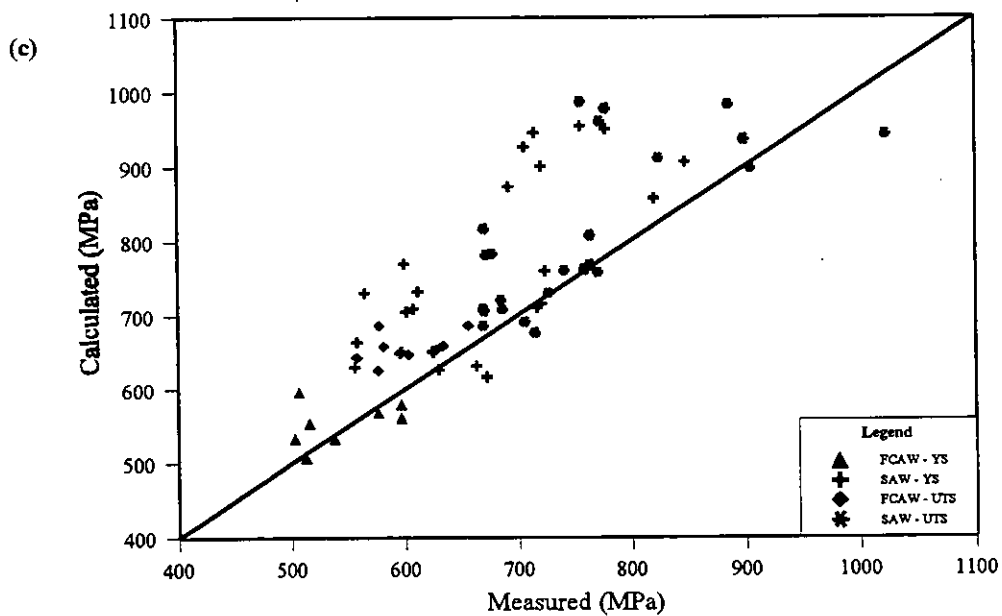
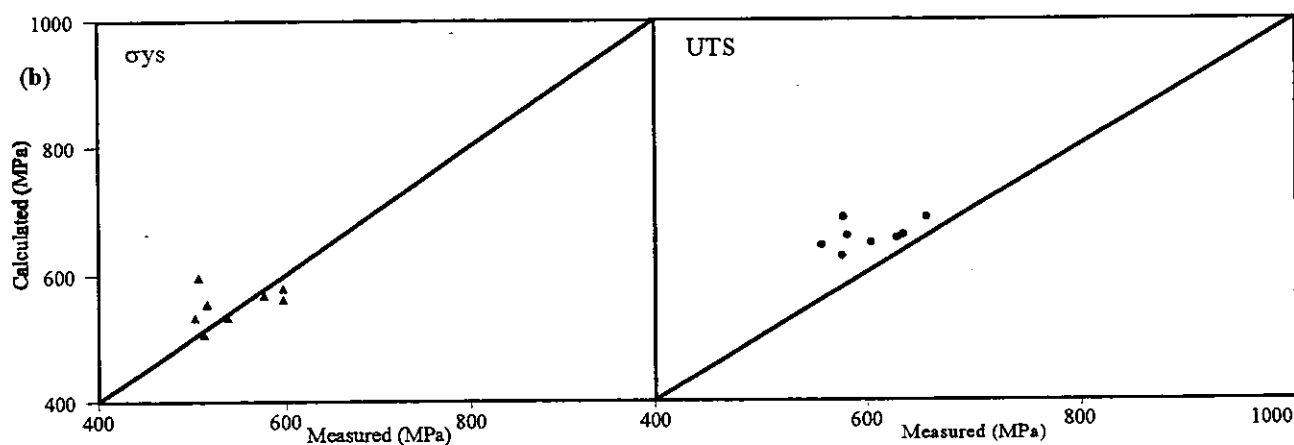
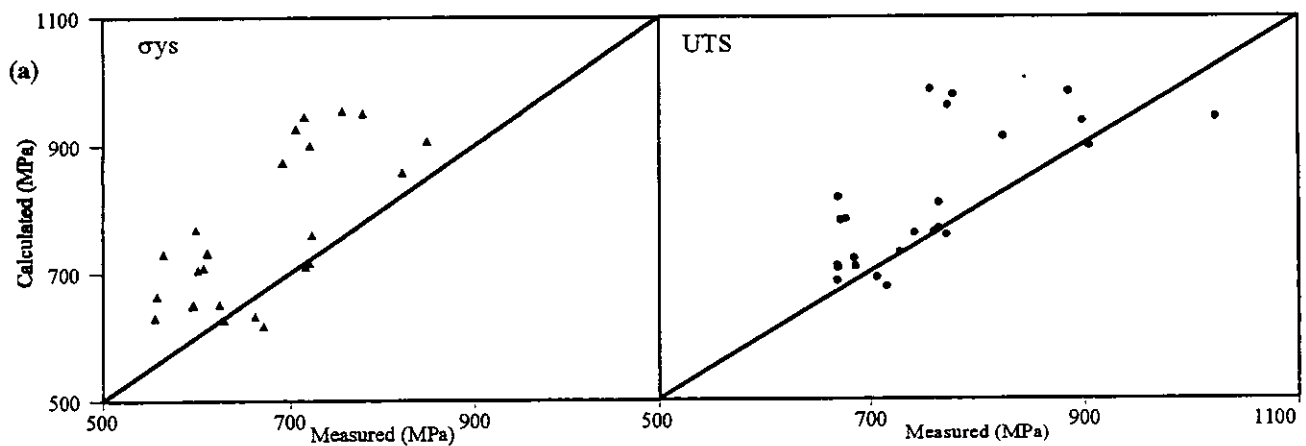


**FIGURE 7** Comparison of measured and calculated model predictions for the yield strength ( $\sigma_{ys}$ ) and UTS for: (a) SAW welds, (b) FCAW welds, and (c) combined data.

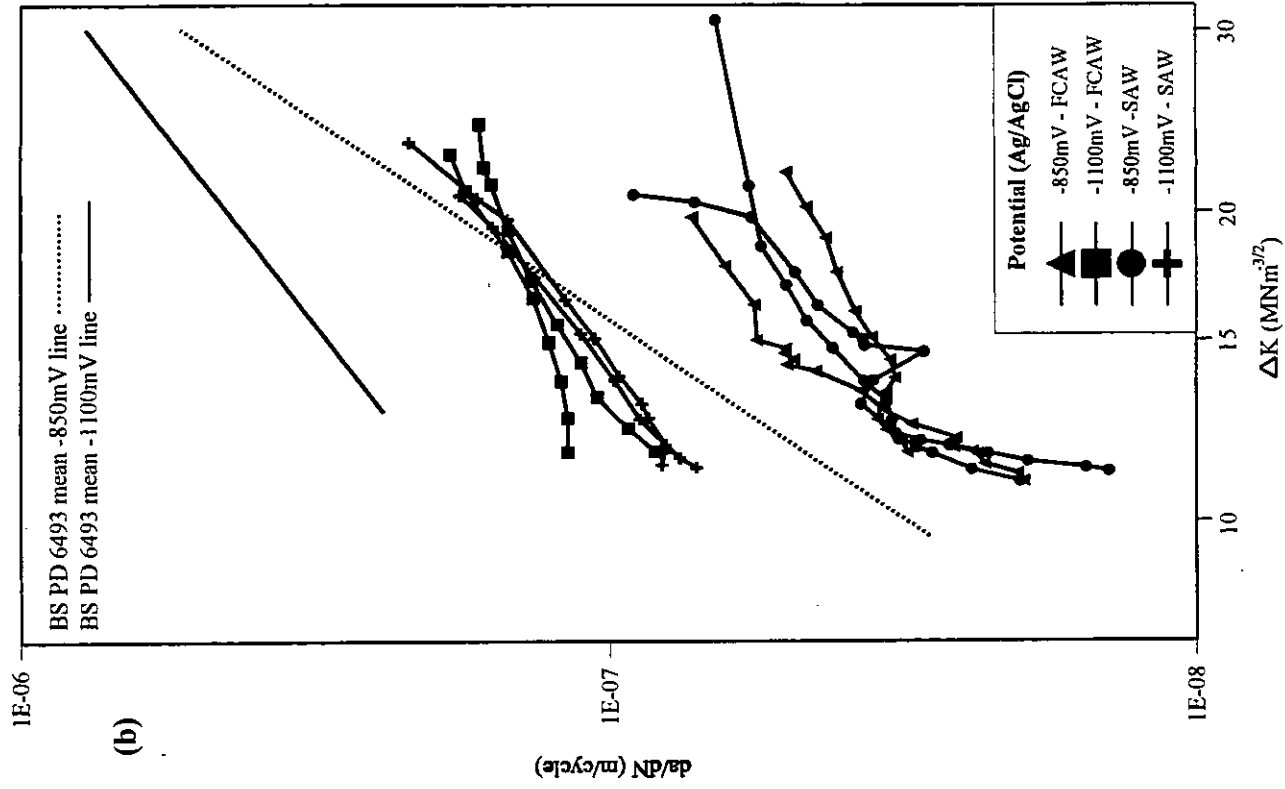
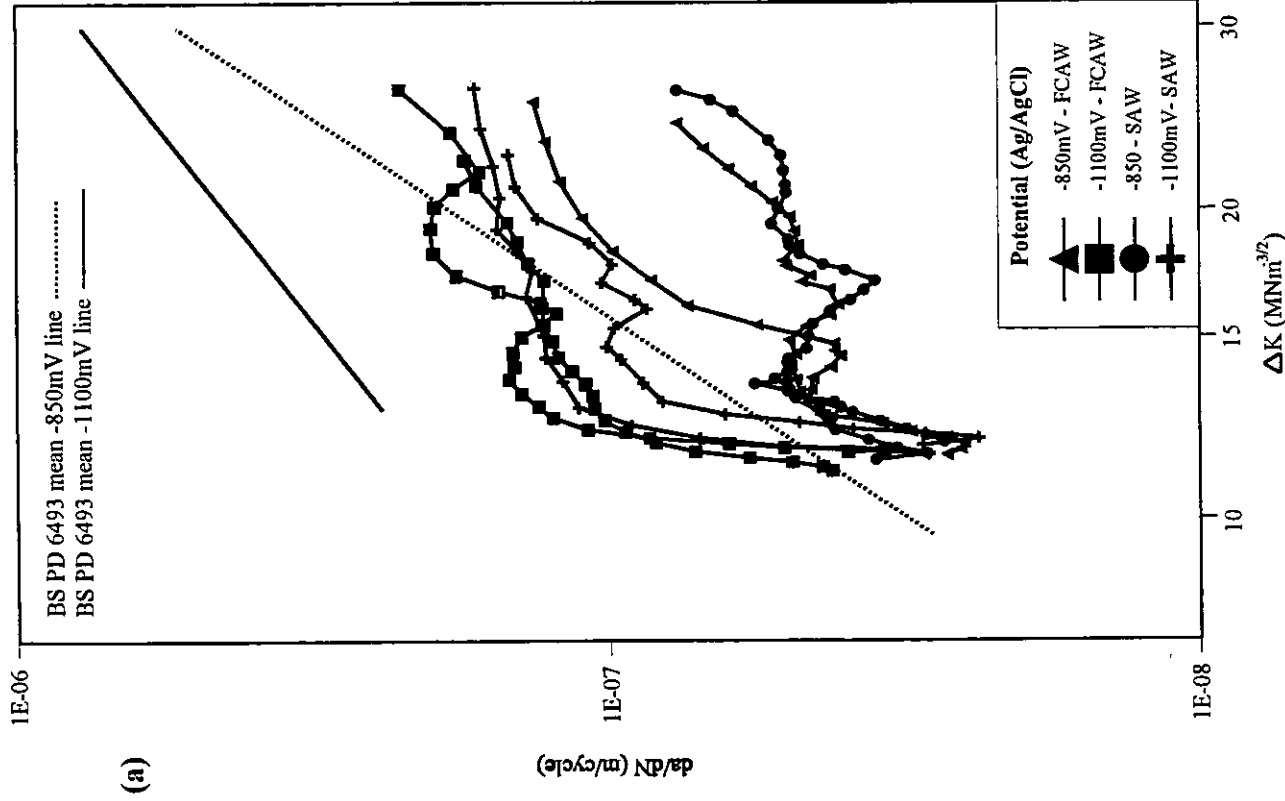


**FIGURE 9** Corrosion fatigue results for: (a) 550MPa and (b) 700MPa steel weld metals at  $-850$  and  $-1100\text{mV}(\text{Ag}/\text{AgCl})$  in artificial seawater at  $R = 0.6$  and  $f = 0.5\text{Hz}$

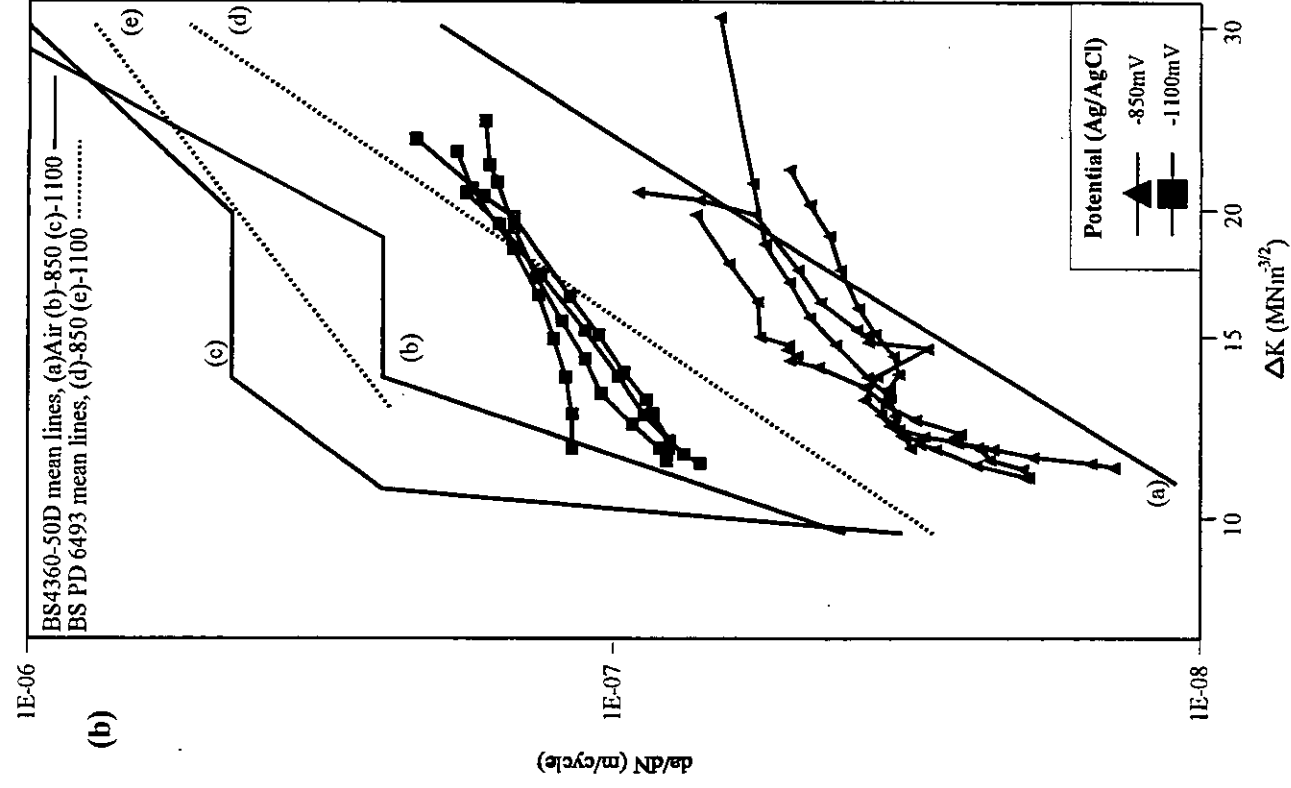
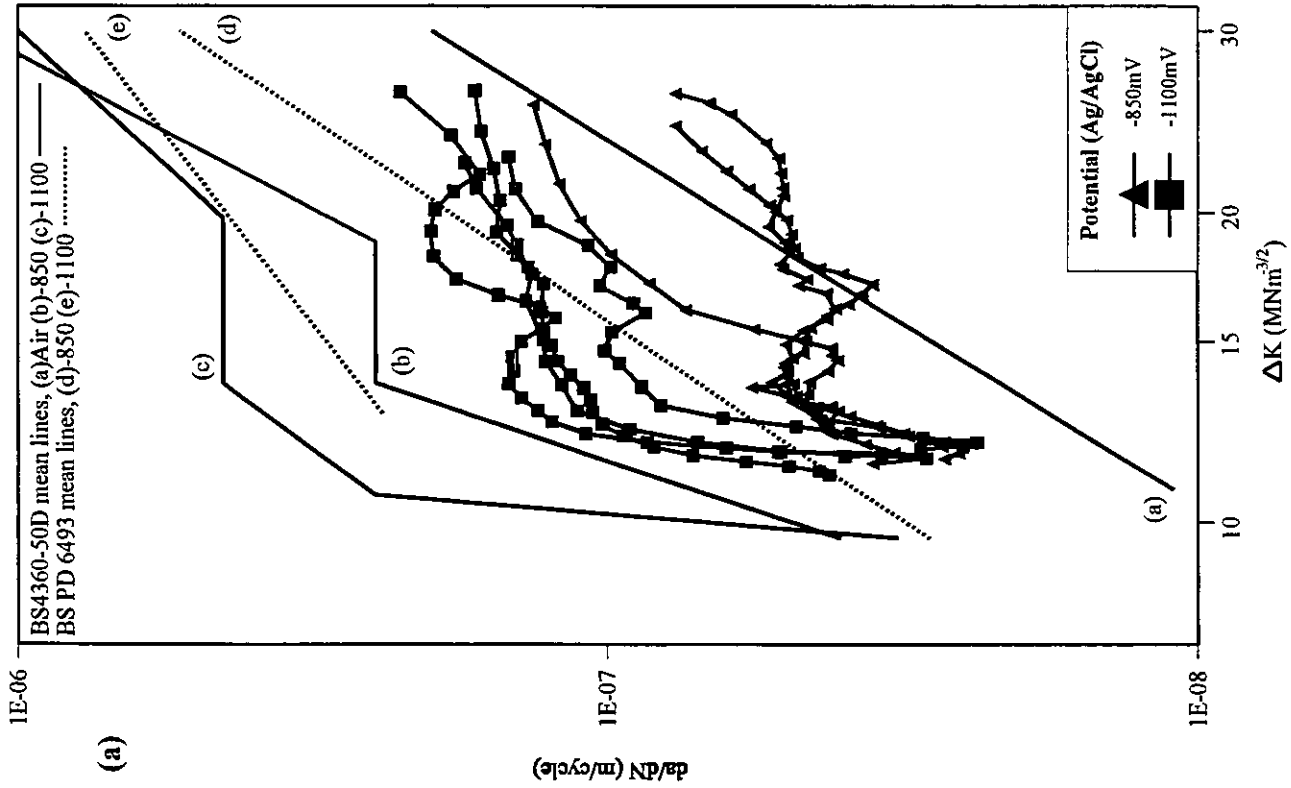


**Figure 10** Corrosion fatigue results for: (a) 550MPa and (b) 700MPa steel weld metals compared to other published corrosion fatigue data under similar experimental conditions



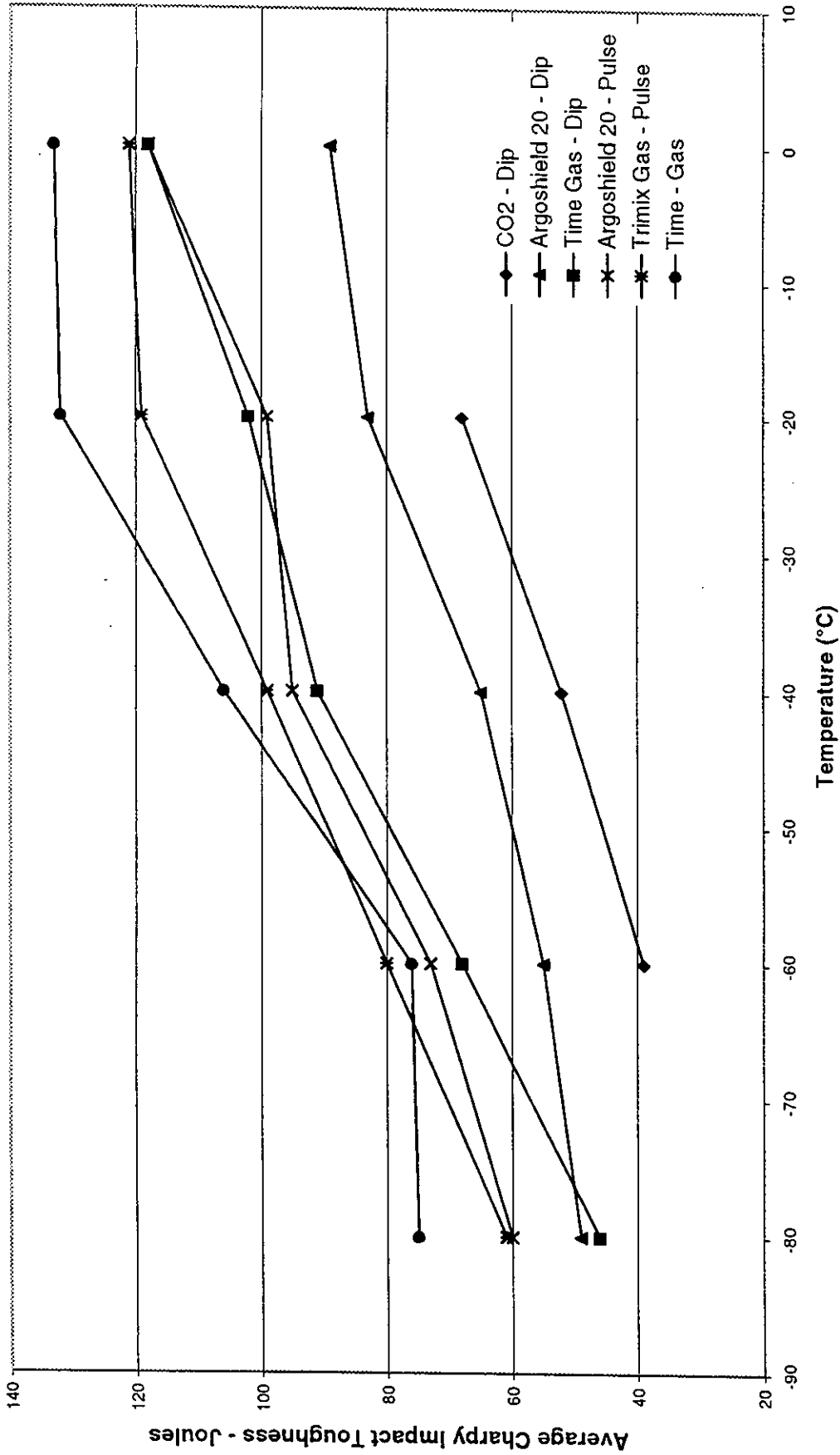


**FIGURE 11** Showing the Charpy-V transition curves for Thyssen Union NiMoCr GMAW Pipeline welding consumable under varying conditions of shielding gas and transfer mode.

